MICROWAVE SPECTROSCOPY OF PENTAFLUOROSULFANYLISOCYNATE

by

Lee-Lee Tho

Thesis submitted to the Faculty of the

Virginia Polytechnic Institute and State University

in partial fulfillment of the requirements for the degree of

Master of Science

in

Chemistry

APPROVED:

J. D. Graybeal, Chairman

P. E. Field

T. C. Ward

May, 1986

Blacksburg, Virginia

MICROWAVE SPECTROSCOPY OF PENTAFLUOROSULFANYLISOCYNATE

by

Lee-Lee Tho

J. D. Graybeal, Chairman

Chemistry

(ABSTRACT)

The microwave spectrum of pentafluorosulfanylisocyanate, $SF_5 - N = C = O$ has been investigated in the 8 GHz to 26 GHz region using a conventional Stark modulated spectrometer. Twenty six transitions have been assigned. A rigid rotor fit was performed by using low J transitions. The spectroscopic constants obtained are A = 2707.69 MHz, B = 1191.22 MHz, and C = 1191.13 MHz. These constants are close to those determined by the electron diffraction study on pentafluorosulfanylisocyanate and to this extent tend to support the bent -N = C = O structure as proposed by the electron diffraction study.

Acknowledgements

I would like to express my sincere gratitude to my advisor, Dr. Jack D. Graybeal, for his unending patience, support, and encouragement. I am thankful for his invaluable advice and enormous help in getting me started and keeping me going. Without his help and understanding, this thesis would have been an impossible task. Also thank you for caring and for always being there to provide a guiding hand and a willing ear, throughout my undergraduate and graduate years at Virginia Tech.

I would like to thank Dr. P.E. Field and Dr. T.C. Ward for serving as my Advisory Committee. Many thanks is extended to my two office-mates, Richard White and Robin Claytor. Thank you Richard for automating the lab and helping me with the computer program. And Robin thanks for cheering me up whenever I am down.

My very special thanks to my parents for their constant love, encouragement, and support. Thank you, Mom and Dad, for always being there when I needed you and for having the confidence in me. The sacrifice you have made for me will always be remembered and appreciated. To my brother, thanks for your love, understanding, and patience.

Table of Contents

List of Illustrations

List of Tables

1.0 Introduction

Several molecules containing the isocyanate group have been studied in the vapor phase for the purpose of structural elucidation by both microwave spectroscopy and electron diffraction. Although the structure of pentafluorosulfanylisocyanate, $SF_5 - N = C = O$ has been determined by electron diffraction, no microwave spectroscopic study has been performed on this molecule.

The -N=C=O bond angle in the isocyanate group and the -N=C=S bond angle in the isothiocyanate for many years have always been assumed to be linear. The electron diffraction investigations of

$$CH_3 - N = C = O \ (methylisocyanate) \ [1]$$

$$H - N = C = O \ (cyanic\ acid) \ [1]$$

$$(CH_3)_3Si - N = C = O \ (trimethylsilylisocyanate) \ [2]$$

$$(CH_3)_3Si - N = C = S \ (trimethylsilylisothiocyanate) \ [2]$$

$$Cl_3Si - N = C = O \ (trichlorosilylisocyanate) \ [3]$$

$$F_3Si - N = C = O \ (trifluorosilylisocyanate) \ [4]$$

$$GeH_3 - N = C = O \ (germylisocyanate)\ [5]$$

$$F_2P - N = C = O \ (difluoroisocyanato\ phosphine)[6]$$

$$F_2P - N = C = S, \ (difluoroisocyanato\ phosphine)[6]$$

all concluded that the N=C=X (X=O,S) structures were linear. Similarly, the microwave studies of

$$CH_3 - N = C = O \ (trimethylisocyante)\ [7][8]$$

$$CH_3 - N = C = S \ (trimethylisothiocyanate)\ [8][9]$$

$$CH_2 = CH - N = C = O, \ (vinylisocyanate)\ [10]$$

$$c - C_3H_5 - N = C = S, \ (cycloproplyisothiocyanate)\ [11]$$

$$SiH_3 - N = C = O \ (silylisocyanate)\ [12]$$

either assumed or indicated that the N=C=X structures are linear.

Recently, both electron diffraction and microwave spectroscopy results have suggested that the -N=C=O bond angle in several isocyanate compounds and the -N=C=S bond angle in several isothiocyanate compounds are bent. Table 1 gives a list of the isocyantes and isothiocyanates, their non-linear bond angles, the techniques from which the results were obtained, and the references of the studies.

Theoretical calculations have also suggested non-linearity in this angle. Various studies have calculated the -N=C=O bond angle to be bent by angles varying from 0.1° to 14.6°. The results of these studies are shown in Table 2. Due to the uncertainties in bond angles calculated by either CNDO/2 or STO-3G calculations it is to be emphasized that these angles are approxi-

Table 1. Previous Experimental Results.

Compounds	< N=C=O	Technique	Reference
$H-N=C=O$	172.6° ± 2.7°	*MW*	[13]
$H-N=C=S$	173.8°*	*MW*	[14]
$Cl-N=C=O$	171.4° ± 1.5°	*MW*	[15]
	169.6°*	*ED + MW*	[16]
$SF_5-N=C=O$	173.8° ± 3.7°	*ED*	[19]
$SeF_5-N=C=O$	172.9 ± 3.2°	*ED*	[19]
$TeF_5-N=C=O$	175.7 ± 2.6°	*ED*	[19]

* No reported deviation.

Table 2. Theoretical Results.

Compounds	< N=C=O	Method	Reference
$H-N=C=O$	172.8°	*CNDO/2*	[18]
	170.0°	*CNDO/2*	[19]
	175.0°	*ab Initio*	[20]
$F-N=C=O$	165.4°	*CNDO/2*	[18]
$Cl-N=C=O$	176.1°	*CNDO/2*	[18]
$F_3C-N=C=O$	174.7°	*CNDO/2*	[21]
$H_3Si-N=C=O$	177.4°	*CNDO/2*	[21]
$F_2P-N=C=O$	179.9°	*CNDO/2*	[21]
$Li-N=C=O$	174.2°	*CNDO/2*	[22]
$SF_5-N=C=O$	172.9°	*STO − 3G*	[23]

mate. However the ab initio work of McLean, Loew, and Berkowitz [20] which involved extensive basis sets is a reliable indication that the -N = C = O angle is bent.

The primary objective of this research was to observe and measure the microwave spectrum of $SF_5 - N = C = O$, and if sufficient data were avaliable determine the molecular structure of $SF_5 - N = C = O$, in order to confirm or reject the structure proposed in the electron diffraction study [15]. It was also anticipated that the dipole moment of $SF_5 - N = C = O$ could be determined if the magnitude of the dipole components and the line intensities were favorable.

2.0 Theory

Microwave Spectroscopy deals mainly with pure rotational motion of molecules in the gaseous state. It covers the frequency range from about 3 GHz to 300 GHz [24]. A molecule must have a permanent dipole moment in order to have a pure rotational spectrum.

From the analysis of the rotational spectrum of a molecule, the principal moments of inertia of that molecule can be obtained. In microwave spectroscopy, the molecule can be classified into 3 categories; linear molecules; symmetric top molecules; and asymmetric top molecules, depending on their principal moments of inertia (I_a, I_b, I_c). Conventionally, $I_a \leq I_b \leq I_c$. Table 3 shows the classification of molecules based on their principal moments of inertia.

Through the methods of quantum mechanics, the discrete rotational energy levels of each type of molecule can be determined. The spectra observed are due to the changes in rotational energies and are governed by selection rules obtained by quantum mechanical methods.

Table 3. Classification of Molecules According to Their Moments of Inertia.

Moment of Inertia	Type of Rotor	Example
$I_a = 0,\ I_b = I_c$	*Linear*	*HCl,*
$I_a = I_b = I_c$	*Spherical*	CH_4, SF_6
$I_a < I_b = I_c$	*Prolate Symmetric*	CH_3I, NH_3
$I_a = I_b < I_c$	*Oblate Symmetric*	C_6H_6, $CHCl_3$
$I_a \neq I_b \neq I_c$	*Asymmetric Top*	H_2O, *HNCO*

2.1 *Asymmetric Top Molecule*

Since the predicted structure of $SF_5 - N = C = O$ is that of a slightly asymmetric top molecule, an overview of the determination of the energy levels for the asymmetric top molecule will be given [24] [25] [26] [27].

An asymmetric top molecule has 3 unequal moments of inertia ($I_a \neq I_b \neq I_c$). Such molecules have more complex pure rotational spectra than symmetric top molecules and the frequencies of these rotational transitions cannot generally be expressed in terms of simple equations.

The asymmetric top molecule is often described by Ray's asymmetry parameter:

$$\kappa = \frac{2B - A - C}{A - C} \qquad [2.1]$$

where the rotational constants are defined as

$$A = \frac{h^2}{8\pi^2 I_a}$$

$$B = \frac{h^2}{8\pi^2 I_b}$$

$$C = \frac{h^2}{8\pi^2 I_c}$$

The limiting values $\kappa = -1$ and $\kappa = +1$, correspond to the prolate and oblate symmetric tops respectively. For an asymmetric top molecule, $-1 < \kappa < +1$. The energy levels of a slightly asymmetric top molecule ($\kappa \cong -1$ and $\kappa \cong +1$) differ from those of the limiting symmetric top molecule in that levels corresponding to $\pm K$, where K is the quantum number specifying the angular momentum about the the symmetry axis, are separated. These levels which are always

degenerate in the symmetric top molecule have the degeneracy removed in an asymmetric top molecule. Therefore, an asymmetric top molecule has (2J + 1) distinct rotational sublevels for each value of J. These sublevels can be designated by several notations. This discussion will use the double subscript system, $J_{K_{-1}K_{+1}}$, of King, Hainer, and Cross [27]. In this notation the first subscript, K_{-1} represents the K value of the limiting prolate symmetric top, while the second subscript, K_{+1} represents the K value of the limiting oblate symmetric top. Another method of labeling the asymmetric top molecule rotational sublevels uses the subscript τ which is related to the K_{-1} and K_{+1} subscripts by

$$\tau = K_{-1} - K_{+1} \qquad [2.2]$$

2.2 *Energy Levels of Asymmetric Top Molecule and Slight Asymmetric Top Molecules*

The classical rotational energy of a molecule is given by

$$E_r = \frac{1}{2}I_x\omega_x^2 + \frac{1}{2}I_y\omega_y^2 + \frac{1}{2}I_z\omega_z^2 \qquad [2.3]$$

where I_x, I_y, and I_z are the principal moments of inertia; and ω_x, ω_y, and ω_z are the angular velocities. Since the angular momentum is related to the angular velocity by

$$P_g = I_g\omega_g \qquad (g = x, y, z) \qquad [2.4]$$

the classical rotational energy can be expressed in terms of the angular momentum

$$E_r = \frac{P_x^2}{2}I_x + \frac{P_y^2}{2}I_y + \frac{P_z^2}{2}I_z \qquad [2.5]$$

The quantum mechanical hamiltonian is given by the expression

$$\mathbf{H}_r = \frac{1}{2}\left(\frac{\mathbf{P}_x^2}{I_x} + \frac{\mathbf{P}_y^2}{I_y} + \frac{\mathbf{P}_z^2}{I_z}\right) \qquad [2.6]$$

where the classical angular momenta have been replaced by the angular momentum operators. The eigenvalues of the hamiltonian matrix are the quantized energies from which the microwave spectral frequencies are determined. The elements of the hamiltonian matrix are given by

$$(J,K,M|\mathbf{H}_r|J'',K'',M'') = \frac{1}{2}(J,K,M|\frac{\mathbf{P}_x^2}{I_x} + \frac{\mathbf{P}_y^2}{I_y} + \frac{\mathbf{P}_z^2}{I_z}|J'',K'',M'') \qquad [2.7]$$

where

J = quantum number specifying the total angular momentum

K = quantum number specifying the component of angular momentum about the molecular symmetry axis

M = quantum number specifying a component of angular momentum about a space fixed z-axis

Each of the squared angular momentum operator on the right hand side can be expressed as a product of the angular momentum matrix elements

$$(J,K,M|\mathbf{P}_g^2|J'',K'',M'') = \sum_{J'}\sum_{K'}\sum_{M'}(J,K,M|\mathbf{P}_g|J'',K'',M'') \times (J,K,M|\mathbf{P}_g|J'',K'',M'') \qquad [2.8]$$

Using the angular momentum matrix elements given in Table 4 the non-zero terms in the energy matrix of an asymmetric top molecule are found to be

$$(J,K,M|\mathbf{H}_r|J,K,M) = \frac{h^2}{16\pi^2}\left[J(J+1)\left(\frac{1}{I_b}+\frac{1}{I_c}\right) + K^2\left(\frac{2}{I_a}-\frac{1}{I_b}-\frac{1}{I_c}\right)\right] \qquad [2.9]$$

$$(J,K,M|\mathbf{H}_r|J,K\pm 2,M) = \frac{h^2}{32\pi^2}[J(J+1) - K(K\pm 1)]^{1/2} \qquad [2.10]$$

$$\times\ [J(J+1)(K\pm 1)(K\pm 2)]^{1/2} \times \left(\frac{1}{I_b}-\frac{1}{I_c}\right)$$

Table 4. Angular Momentum Matrix Elements.

Angular Momentum Matrix Elements
$(J,K,M \mid \mathbf{P}_z \mid J,K,M) = \frac{h}{2\pi} K$
$(J,K,M \mid \mathbf{P}_y \mid J,K \pm 1,M) = \mp i \frac{h}{2\pi} (J,K,M \mid \mathbf{P}_x \mid J,K \pm 1,M)$ $= h(\frac{1}{4\pi}) [J(J+1) - K(K \pm 1)]^{1/2}$
$(J,K,M \mid \mathbf{P}^2 \mid J,K,M) = \frac{h^2}{4\pi^2} J(J+1)$
$(J,K,M \mid \mathbf{P}_z^2 \mid J,K,M) = \frac{h^2}{4\pi^2} K^2$
$(J,K,M \mid \mathbf{P}_y^2 \mid J,K,M) = (J,K,M \mid \mathbf{P}_x^2 \mid J,K,M)$ $= \frac{h^2}{8\pi^2} [J(J+1) - K^2]$
$(J,K,M \mid \mathbf{P}_y^2 \mid J,K \pm 2,M) = -(J,K,M \mid \mathbf{P}_x^2 \mid J,K \pm 2,M)$ $= \frac{h^2}{8\pi^2} [J(J+1) - K(K \pm 1)]^{1/2}$ $\times [J(J+1) - (K \pm 1)(K \pm 2)]^{1/2}$

Since non-zero elements occur only for

$$J'' = J$$

$$K'' = K, K \pm 2$$

$$M'' = M$$

there are no off diagonal matrix elements in J, or M (the energy is independent of the spacial orientation of **P**), and the energy matrix can be factored into J-blocks which may be solved separately (see Figure 1). Thus, for each J value there is a matrix of order 2J + 1.

King, Hainer and Cross [27] have shown that by means of the Wang symmetry transformation, the elements in each of the J blocks of the energy matrix can be converted to an expression which contains a diagonal term which depends only on J and an off diagonal term which is a function of the energy level and κ. The rotational energy, $E^J_{K,K'}$, thus becomes

$$E^J_{K,K'} = \frac{1}{2}(A + C)J(J + 1) + \frac{1}{2}(A - C)E^J_{K,K'}(\kappa) \qquad [2.11]$$

where

A, B, C = rotational constants

$E^J_{K,K'}(\kappa)$ = reduced energy matrix element which depends on the asymmetry

κ = Ray's asymmetry parameter

The reduced energy matrix is diagonal in J, but not in K. The nonvanishing matrix elements of $E^J_{K,K'}(\kappa)$ are [26]

$$E^J_{K,K} = (J,K,M|\mathbf{H}(\kappa)|J,K,M) = F[J(J + 1) - K^2] + GK^2 \qquad [2.12]$$

$$E^J_{K,K\pm 2} = (J,K,M|\mathbf{H}(\kappa)|J,K \pm 2,M) = H[f(J,K \pm 1)]^{1/2} \qquad [2.13]$$

where

$$f(J, K \pm 1) = \frac{1}{4}[J(J+1) - K(K \pm 1)][J(J+1) - (K \pm 1)(K \pm 2)] \qquad [2.14]$$

Furthermore, the matrix elements have the following relationships

$$E_{K,K} = E_{-K,-K}$$

$$E_{K,K+2} = E_{K+2,K} = E_{-K,-K-2} = E_{-K-2,-K}$$

The constants F, G, and H depend on the particular way in which the a, b, and c axes are identified with the x, y, and z axes [26]. There are 6 possible ways to make this identification.

For a slightly prolate top, like $SF_5 - N = C = O$, where the a axis is identified with the z axis, the b axis with the x axis, the c axis with the y axis and $\kappa \cong -1$, these constants have values of

$$H = -\frac{1}{2}(\kappa + 1), \quad G = 1, \quad F = \frac{1}{2}(\kappa - 1)$$

Therefore the diagonal matrix elements are given by

$$\frac{1}{2}(\kappa - 1)J(J+1) - \frac{1}{2}(\kappa - 3)K_{-1}^2$$

and the off diagonal matrix elements are given by

$$-\frac{1}{2}(\kappa + 1)\left[\frac{1}{4}[J(+1) - K(K_{-1} \pm 1)][J(J+1) - (K_{-1} \pm 1)(K_{-1} \pm 2)]\right]^{1/2}$$

This $E^J_{K,K}(\kappa)$ matrix forms a basis for a secular determinant, $|E^J_{K,K}(\kappa) - I\lambda| = 0$, where I is a unit matrix, and the λ are the allowed reduced energy terms for an asymmetric top molecule. The roots from the secular determinant, when incorporated into equation [2.11], will give the energy of the molecule as a function of κ.

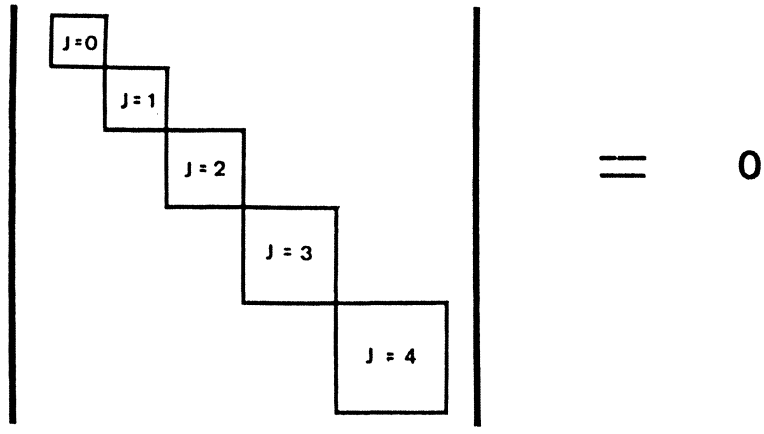

Figure 1. The Energy Matrix Factored Into J-Blocks.

2.3 *Selection Rules*

The selection rules for an asymmetric top molecule are more complex than for a symmetric top molecule. They not only involve the quantum number J, but also the pseudo quantum numbers, K_{-1} and K_{+1}.

The allowed changes in J for dipole absorption of radiation in an asymmetric top molecule are the same as those for a symmetric top molecule,

$$\Delta J = 0, \pm 1.$$

These "permitted" transitions result from the nonvanishing property of the dipole matrix element when $J' = J$ or $J' = J \pm 1$. For other values of J', all matrix elements of the dipole components along space fixed axes are zero [13]. The transitions due to $\Delta J = 0$ are designated as "Q - branch" transitions, those due to $\Delta J = +1$ as "R - branch" transitions, and those due to $\Delta J = -1$ as "P - branch" transitions.

The restrictions imposed by K_{-1} and K_{+1} also play an important role in the selection rules. These restrictions can be derived from the symmetry properties of the Four Group V (D_2) [25] [26] [28] [29].

If the dipole moment lies wholly along one of the principal axes, only those changes in the subscripts K_{-1} and K_{+1} corresponding to that component are allowed. If there are dipole components along all 3 of the principal axes, then all 3 changes listed in Table 5 are allowed. The transitions resulting from the μ_g component are designated as "g - type" transitions, (g = a, b, c). The presence of all more than one type of transition in an asymmetric top molecules makes the spectrum more complex. A summary of these selection rules are given in Table 5.

Table 5. Selection rules for an asymmetric top.

μ_g (g = a,b,c)	ΔJ	ΔK_{-1}	ΔK_{+1}
μ_a	0, ± 1	0, ± 2, ...	± 1, ± 3, ...
μ_b	0, ± 1	± 1, ± 3, ...	± 1, ± 3, ...
μ_c	0, ± 1	± 1, ± 3, ...	0, ± 2, ...

2.4 *Determination of Dipole Moments By the Stark Effect*

The Stark effect provides a very accurate and convenient method for determining the magnitude of molecular dipole moments. This is done by measuring the frequency shifts of lines in the applied electric field of a Stark modulated spectrometer. For such measurement, a uniform known electric field is needed, and the spectral assignments of the transitions must be known.

The frequency displacement of a stark component can be expressed as a function of the electric field strength by the following relationship,

$$\Delta\nu = (A' + M^2A'')\mu_a^2\varepsilon^2 + (B' + M^2B'')\mu_b^2\varepsilon^2 + (C' + M^2C'')\mu_c^2\varepsilon^2 \qquad [2.15]$$

where $A', A'', B', B'', C',$ *and* C'' are the stark coefficients. For $\Delta\nu$ in MHz μ_g is in Debye units, and ε is in volts/cm. If the observed values of $\Delta\nu$ versus E^2 , for several known transitions are plotted, the slopes of the resulting lines may be used to evaluate the dipole moment components, μ_g. A more detail description of this relationship is given in ref. [26].

3.0 Experimental

3.1 Instruments

The microwave spectrometer used in this investigation was a conventional Stark modulated spectrometer. Transitions in the frequency range of 8 GHz to 26 GHz were measured.

The microwave source was the Hewlett-Packard 8673B Synthesized Signal Generator with a frequency range of 2 GHz to 26 GHz. This source can be operated manually, as well as using a Hewlett-Packard 200 Series computer system. The monochromatic microwave radiation from this source was absorbed by the compound in the sample cell. The sample cell was a ten foot long X - band or P - band copper waveguide with a Stark electrode fitted along its length, and with mica windows at the ends. The Stark electrode is parallel to and equidistant from the wide faces of the waveguide [30]. A square wave with a frequency of $\cong 33KHz$ from the Stark modulator was applied to the Stark electrode.

The absorption of the microwave radiation by the sample was detected using appropriate Hewlett Packard crystal detectors. The signal from the crystal detector was sent into a preamplifier

and then to a EG & G 5207 Lock-In Amplifier. The output from the Lock-In Amplifier was recorded by a Fisher Recordall Series 5000 chart recorder. The Lock-In Amplifier was also interfaced to the Hewlett-Packard 200 Series computer system, where the output was stored on floppy diskettes. A hardcopy of the results can also be plotted out, and the frequency of each peaks can be measured accurately from the computer. This computer system consists of a HP82913A monitor; a HP9133 disk drive; a HP 9000 central processing unit; and a HP 7475A plotter. A block diagram of the spectrometer is given in Figure 2.

3.2 Sample

The $SF_5 - N = C = O$ sample was provided by Dr. J. S. Thrasher of the University of Alabama. It was prepared from NSF_3 *and* COF_2 in the presence of HF [31],

$$NSF_3 \; + \; COF_2 \xrightarrow{HF} SF_5 - N = C = O$$

$SF_5 - N = C = O$ is a colorless, low boiling liquid $(5°C - 5.5°C)$ [36] with moderate chemical reactivity. NSF_3 was found to be present as an impurity in the sample. The transitions due to NSF_3 were found at the frequencies reported in the literature [36] and are listed in Table 6.

3.3 Spectra

The microwave spectrum of $SF_5 - N = C = O$ was recorded at a temperature of $\cong 233°K$; a pressure of 50 mTorr and over the frequency range of 8 GHz to 26 GHz. The spec-

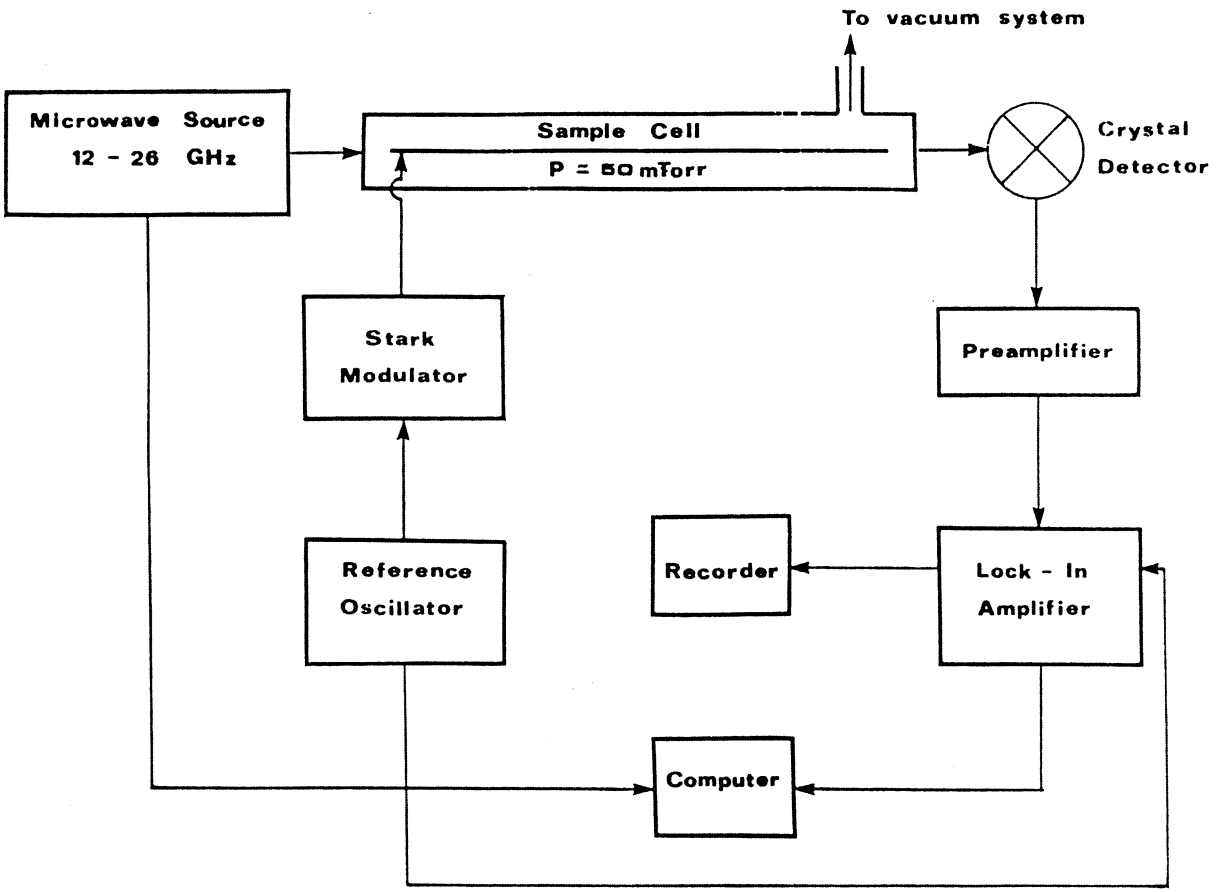

Figure 2. A schematic block diagram of the Stark modulated spectrometer.

Table 6. The Observed Frequencies Of The Thionitrosyl(V) Fluoride.

Observed Frequency (MHz)
9275.5
18522.25
18545.38

trum was recorded in the range of 8 GHz to 18 GHz using a "X-band" Stark cell, and in the range from 12 GHz to 26 GHz using a "P-band" Stark cell.

The frequencies of the transitions were measured in two ways. Initially they were observed on the output of the chart recorder and measured by manually setting the source to the frequency of the transition. Latter work involve plotting the spectrum onto the monitor of the computer, and using the cursor set on a peak to determine the frequency directly.

A total of 501 rotational transitions of the $SF_5 - N = C = O$ have been measured. Table 7 lists the observed frequencies and intensities of the transitions measured at a Stark voltage of 200V. The observed frequencies and intensities of those measured at a Stark voltage of 800V are listed in Table 8, 9, 10, 11, 12, and 13.

Frequencies of the Stark components of one transition at 9403.76 MHz were measured at Stark levels of 200V, 400V, 600V, and 800V. It is observed that the Stark peak moves towards higher frequencies, as the Stark voltage is changed from 200V to 800V. Only the impurity peak in this range was observed when the Stark voltage was 200V. Table 14 shows these shifts in frequencies.

Table 7. Observed Frequencies And Intensities At 200V.

Observed Frequency (MHz)	Relative Intensity	Observed Frequency (MHz)	Relative Intensity
8911.55	1.5	20335.41	1.5
9403.67	2.4	20427.07	1.8
10278.39	13.2	20460.30	3.3
11788.78	1.2	20477.79	1.0
12131.95	2.0	20504.01	1.8
12257.25	2.5	21170.59	3.0
14319.38	1.8	21631.95	2.4
14588.13	2.0	21952.64	2.5
16307.25	2.3	22234.50	1.5
16681.25	2.8	22482.50	4.4
16913.13	1.8	23035.00	1.0
16938.22	1.2	23190.40	1.0
17575.75	2.6	23414.30	4.7
17605.13	2.1	23654.50	4.5
18478.00	6.0	23714.69	1.1
18514.50	15.5	23732.92	3.3
18583.50	5.0	24039.50	6.0
18654.75	12.7	24083.00	2.3
18850.38	3.2	25049.63	2.3
18971.57	6.0	25393.00	5.1
19226.63	2.1	25521.50	1.0
19636.38	2.0	25676.53	1.5

Table 8. Observed Frequencies And Intensities At 800V.

Observed Frequency (MHz)	Relative Intensity	Observed Frequency (MHz)	Relative Intensity
8421.00	18.7	13441.00	3.0
8578.75	6.5	13457.53	2.0
8912.13	34.0	13461.13	2.3
9403.50	32.1	13475.75	1.8
10278.88	57.0	13484.57	4.0
11788.88	2.8	13488.00	2.0
11789.25	16.0	13499.75	2.5
12017.50	7.0	13510.17	4.8
12042.40	4.5	13546.90	14.0
12044.96	3.0	13600.90	1.8
12050.40	3.0	13645.00	2.5
12057.98	3.2	13648.13	2.5
12069.48	3.6	13653.15	5.5
12075.38	3.0	13673.14	3.9
12087.08	5.0	13685.26	3.0
12101.63	5.0	13692.63	2.5
12114.78	5.0	13700.57	3.7
12121.30	5.0	13706.38	2.8
12132.64	21.7	13752.88	2.0
12146.45	4.4	13768.00	2.0
12156.10	4.5	13794.06	5.2
12163.55	3.0	13806.50	5.0
12179.45	3.5	13830.30	2.0
12258.00	40.4	13848.87	4.3
12266.80	5.0	13852.05	3.5
12344.38	4.5	13858.30	3.1
12547.30	2.0	13874.29	5.0
12553.18	2.0	13888.10	2.0
12618.70	3.0	13904.38	2.0
12778.00	2.8	13908.80	5.5
12862.20	8.5	13914.06	9.7
12937.90	2.5	13918.86	8.0
12999.00	2.6	13922.74	4.0
13119.93	4.0	13930.75	1.5
13185.50	2.8	13946.75	2.0
13153.83	4.0	13950.65	6.0
13171.33	6.0	13962.88	1.8
13208.75	2.5	13970.74	5.0
13220.45	1.3	14031.31	2.3
13264.63	1.4	14039.90	4.0
13282.73	2.0	14180.07	2.5
13290.20	4.0	14197.71	3.7
13428.57	2.0	14233.14	2.5
13437.71	3.0	14250.29	4.5

Table 9. Observed Frequencies And Intensities At 800V. (Cont.)

Observed Frequency (MHz)	Relative Intensity	Observed Frequency (MHz)	Relative Intensity
14261.40	13.7	15608.90	10.0
14267.89	4.0	15613.83	5.0
14279.10	20.0	15615.65	7.0
14293.90	4.1	15621.43	6.5
14320.40	12.0	15626.48	2.5
14323.66	4.3	15633.80	5.0
14350.70	10.0	15635.20	8.8
14421.68	7.0	15636.15	4.8
14489.56	8.0	15638.15	6.0
14515.40	3.5	15639.48	5.0
14588.38	25.0	15640.83	8.0
14598.68	11.6	15642.35	10.0
14630.35	4.0	15645.03	7.0
14718.30	2.5	15681.70	7.8
14727.30	4.1	15707.38	2.5
14751.43	3.0	15728.80	2.0
14933.50	3.0	15750.98	4.0
14941.13	2.0	15809.18	3.5
14993.25	2.5	15830.18	12.5
15045.08	5.0	15865.15	15.0
15079.25	7.0	15891.25	12.0
15104.10	13.0	15913.85	5.0
15115.35	14.0	15963.30	26.0
15118.88	9.5	16009.25	8.0
15126.68	3.5	16021.60	4.0
15128.18	9.0	16040.45	46.0
15130.08	5.5	16049.25	2.3
15131.63	3.5	16127.25	1.8
15134.38	5.0	16196.08	8.0
15147.08	5.5	16240.80	3.3
15149.43	3.5	16268.75	2.3
15151.50	4.0	16289.88	26.0
15152.55	4.0	16305.15	27.0
15152.55	4.0	16418.18	25.0
15154.15	4.0	16427.03	4.0
15156.15	5.0	16436.43	17.0
15161.68	18.0	16442.90	18.0
15263.20	6.0	16462.23	12.0
15321.55	7.0	16480.20	17.0
15382.50	5.5	16492.90	14.0
15488.05	12.0	16520.40	13.0
15531.97	4.0	16530.43	10.5
15535.43	6.0	16551.65	6.0
15606.60	6.5	16571.30	11.0

Table 10. Observed Frequencies And Intensities At 800V. (Cont.)

Observed Frequency (MHz)	Relative Intensity	Observed Frequency (MHz)	Relative Intensity
16596.68	24.0	17729.68	25.5
16667.73	6.0	17756.34	1.8
16681.68	31.0	17779.05	5.5
16689.40	37.0	17814.15	6.0
16727.06	28.0	17835.25	17.0
16784.53	6.0	17863.50	40.0
16852.08	20.5	17882.18	20.0
16893.90	2.8	17913.13	12.0
16913.55	30.6	17970.88	3.0
16941.38	36.5	17974.86	2.3
17032.78	8.6	17976.05	18.0
17104.30	28.5	17993.10	13.5
17120.93	10.0	18007.68	40.0
17144.28	12.5	18041.10	6.0
17154.25	16.5	18048.18	12.0
17180.83	8.0	18056.68	21.0
17196.05	19.0	18068.25	10.5
17221.98	21.5	18101.35	37.0
17230.80	12.0	18140.78	8.5
17257.14	3.1	18179.15	37.5
17262.85	33.0	18195.25	20.0
17281.05	15.0	18206.85	25.0
17311.20	15.0	18242.55	13.0
17316.90	30.0	18259.98	14.0
17321.00	42.0	18262.40	3.0
17333.50	52.0	18277.65	28.0
17413.25	32.0	18292.57	3.0
17417.90	21.5	18297.08	9.5
17426.33	23.0	18312.68	17.0
17430.80	11.0	18341.08	7.0
17449.08	11.0	18356.43	48.0
17454.40	15.0	18397.05	20.0
17461.94	4.2	18416.50	16.5
17466.68	10.0	18445.68	27.0
17480.33	38.0	18478.81	21.1
17499.20	8.0	18485.62	26.4
17540.63	6.0	18515.70	12.0
17544.30	13.0	18522.25	7.5
17556.35	11.0	18546.13	52.0
17570.38	40.0	18558.98	52.0
17584.20	40.0	18583.68	55.0
17597.90	40.0	18610.93	15.0
17609.40	27.0	18615.13	27.0
17631.63	41.0	18627.58	12.0

Table 11. Observed Frequencies And Intensities At 800V. (Cont.)

Observed Frequency (MHz)	Relative Intensity	Observed Frequency (MHz)	Relative Intensity
18635.15	15.0	19379.88	65.5
18651.00	43.0	19391.38	60.0
18656.03	43.0	19407.78	7.0
18666.95	43.0	19426.50	30.0
18675.57	4.6	19433.65	13.0
18714.83	17.0	19436.03	7.0
18751.60	6.0	19455.88	25.0
18758.08	20.0	19458.90	20.0
18764.03	18.0	19461.78	29.0
18779.93	10.0	19468.03	37.0
18815.50	23.0	19493.03	4.7
18847.53	32.0	19513.40	10.0
18861.53	50.0	19568.58	16.7
18881.78	12.0	19586.53	24.5
18908.23	4.5	19601.83	13.0
18917.30	6.0	19619.75	14.9
18922.62	10.4	19636.54	26.0
18947.93	7.0	19647.65	4.0
18966.30	37.0	19664.18	8.5
18976.08	16.0	19681.38	2.3
19010.45	9.0	19687.55	37.0
19026.05	60.0	19707.48	37.5
19058.29	7.0	19712.00	4.0
19061.05	57.0	19720.88	20.5
19075.15	5.0	19739.80	39.0
19123.50	15.0	19751.35	28.0
19146.38	4.0	19757.60	6.0
19154.28	30.0	19767.75	12.0
19163.63	24.4	19780.50	10.0
19175.68	19.0	19797.43	8.0
19183.50	10.0	19857.90	43.0
19186.73	8.4	19877.85	31.5
19193.53	19.0	19897.13	2.3
19208.88	34.5	19923.15	51.0
19216.58	12.0	19925.50	2.0
19225.70	8.0	19938.00	4.0
19275.43	6.3	19956.48	38.0
19278.30	4.0	19962.38	2.8
19290.70	14.0	20134.60	1.2
19320.25	2.3	20145.80	1.6
19328.59	5.2	20335.38	52.0
19344.45	60.0	20357.30	2.5
19357.45	55.0	20427.13	1.8
19363.21	6.6	20460.75	38.0

Table 12. Observed Frequencies And Intensities At 800V. (Cont.)

Observed Frequency (MHz)	Relative Intensity	Observed Frequency (MHz)	Relative Intensity
20477.25	3.3	22084.38	3.5
20507.13	3.1	23036.25	29.3
20519.50	5.5	23170.00	4.5
20571.40	4.5	23178.75	2.8
20651.75	2.2	23193.75	6.0
20700.50	2.2	23280.63	8.8
20792.60	3.8	23316.25	3.8
20834.63	3.0	23395.63	3.5
20881.42	4.0	23414.78	31.7
20931.63	2.3	23418.13	51.9
21083.13	1.5	23460.63	6.5
21171.38	6.5	23480.50	7.3
21188.73	7.1	23495.00	4.5
21197.34	22.0	23511.25	6.5
21207.63	3.5	23543.75	5.0
21224.13	5.0	23556.25	5.8
21370.38	3.0	23573.13	9.8
21385.88	2.6	23606.25	5.5
21451.75	3.8	23612.41	6.8
21568.00	3.0	23658.85	8.5
21632.64	8.0	23715.16	7.2
21662.10	6.3	23822.58	7.5
21801.00	2.6	23870.50	6.3
21824.00	2.5	23893.13	7.2
21871.13	2.5	23915.66	5.0
21901.38	3.0	23967.70	7.0
21955.75	2.0	23971.25	10.8
22066.25	7.8	24010.50	4.8
22085.00	3.8	24041.88	52.0
22111.25	4.0	24086.88	52.0
22163.75	3.3	24118.75	5.0
22222.50	4.3	24123.13	3.0
22236.25	50.0	24191.88	5.3
22270.00	3.3	24259.10	2.6
22308.38	25.3	24260.63	3.5
22452.50	2.0	24321.88	18.0
22483.85	50.0	24471.00	3.0
22528.60	6.1	24668.76	3.0
22695.00	6.3	24786.88	3.3
22738.13	6.7	24821.25	5.1
22908.75	9.2	24852.50	4.0
22933.75	3.6	24927.50	3.0
22960.30	3.9	24480.00	4.8
22966.23	4.1	25052.50	52.0

Table 13. Observed Frequencies And Intensities At 800V. (Cont.)

Observed Frequency (MHz)	Relative Intensity	Observed Frequency (MHz)	Relative Intensity
25096.25	7.0	25627.07	5.0
25120.00	2.0	25676.42	8.2
25126.25	4.0	25683.13	4.5
25158.13	3.0	25713.75	5.0
25172.50	14.5	25750.75	6.3
25321.88	6.5	25810.00	7.0
25326.23	9.0	25908.49	6.0
25346.60	5.0	25913.75	3.8
25396.25	52.0	26030.00	2.0
25456.25	5.5	26038.75	7.3
25465.04	4.0	26115.66	5.0
25471.25	6.5	26150.00	4.5
25486.88	6.0	26245.09	8.0
25522.18	6.6	26407.41	11.0
25526.26	5.8	26489.38	5.5
25555.00	1.8	26500.00	12.2
25572.50	2.3		

Table 14. Stark Effect Of The 9403.76 MHz Transition.

Stark Voltage	200V	400V	600V	800V
Line Peak	-	9403.65	9403.70	9403.95
Stark Peak	-	9406.05	9409.50	9415.15

4.0 Discussion

Prior to analyzing the spectrum of $SF_5 - N = C = O$, a tentative spectrum of possible transitions in the frequency range of 6 GHz to 26 GHz was calculated. To obtained this information, the structural parameters of $SF_5 - N = C = O$ reported in the electron diffraction study by Oberhammer, Seppelt, and Mews [17] were used. Table 15 lists the structural parameters of $SF_5 - N = C = O$ used for the calculated spectrum. The proposed structure from the electron diffraction study is presented in Figure 3.

4.1 Effect of changes in bonding parameters

The bonding parameters from the electron diffraction study were used to calculated the rotational constants (A, B, C) and the Ray's asymmetry parameter (κ). In addition to calculating this set of parameters, four other sets were computed by taking into consideration the reported experimental errors. Since this was a preliminary calculation designed to approximately bracket a range of value for A, B and C, it was not considered to be necessary to select rigorously determine a maximized set but rather the sets were intuitively chosen based on observations of the manner in

Table 15. Bonding Parameters From Electron Diffraction Study.

$SF_5 - N = C = O$	
$N = C$	1.230 ± 0.008 Å
$C = O$	1.179 ± 0.007 Å
$(S - F)_{av}$	1.567 ± 0.002 Å
$S - N$	1.668 ± 0.006 Å
$< S - N = C$	124.9 ± 1.2°
$< N = C = O$	173.8 ± 3.7°

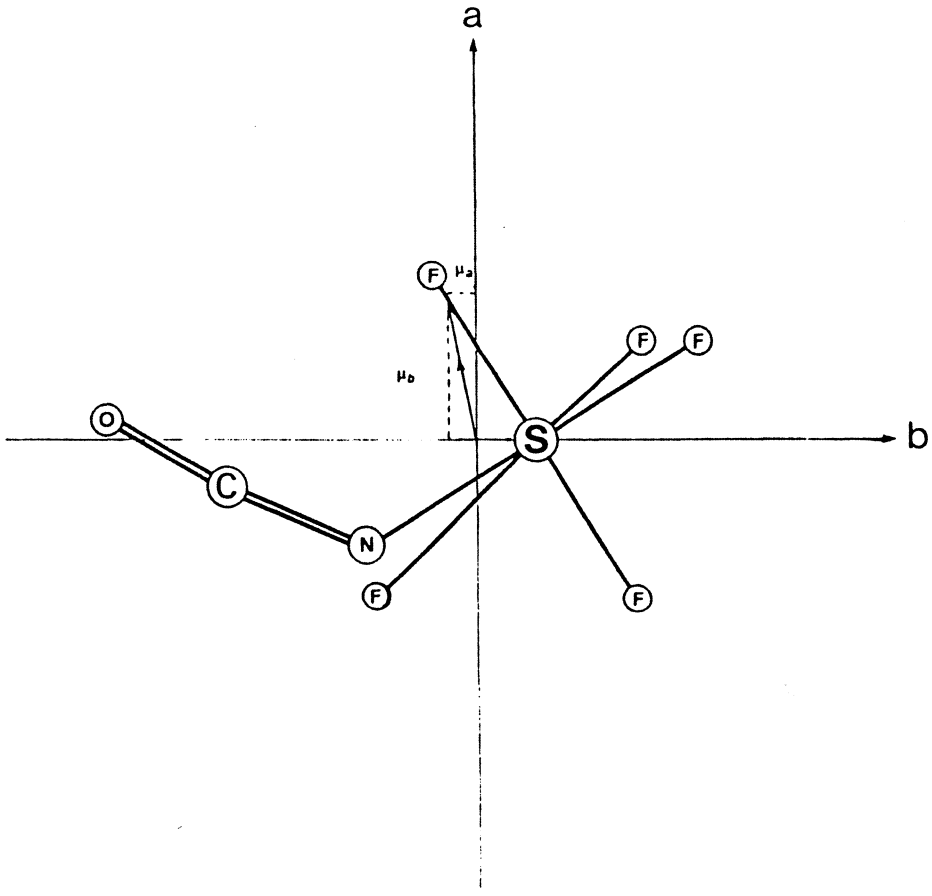

Figure 3. Proposed Structure From Electron Diffraction.

Table 16. Effects Of Changes In Bonding Parameters On Rotational Constants and Ray's Asymmetry Parameter.

	Electron Diffraction	Model 1	Model 2	Model 3	Model 4
$(S - F)_{av}$ (Å)	1.567 ± 0.002	1.569	1.569	1.565	1.565
$S - N$ (Å)	1.668 ± 0.006	1.674	1.674	1.662	1.662
$N = C$ (Å)	1.234 ± 0.008	1.242	1.242	1.226	1.226
$C = O$ (Å)	1.179 ± 0.007	1.186	1.186	1.172	1.172
$< SNC$ (°)	124.9 ± 1.2	126.1	123.7	126.1	123.7
$< NCO$ (°)	173.8 ± 3.7	177.5	170.1	177.5	170.1
A	2704.68	2701.57	2691.66	2717.02	2707.49
B	1192.58	1167.23	1202.82	1184.33	1219.88
C	1191.88	1167.20	1200.88	1184.00	1218.31
kappa	-0.99907	-0.99996	-0.99740	-0.99956	-0.99790

which A, B and C changed relative to individual bond parameter changes. These calculations indicated that the changes in the A, B and C values due to changes in the bonding parameters. Table 16 summarizes this effect.

4.2 *Calculated Spectrum and Stark Effects*

A low resolution sweep was carried out and no strong ${}^{b}Q$ or ${}^{a}R$ branch transitions were observed. This indicates that $\mu < 0.5D$. The μ_c component will be zero since $SF_5 - N = C = O$ has an ab - plane of symmetry. By using dipole moment components of $\mu_a = \mu_b = 0.5D$ together with the previously calculated rotational constants, the possible transitions in the rotational spectrum were calculated.

The $SF_5 - N = C = O$ calculated spectrum was very rich. The calculated spectrum indicated the presence of several narrow clusters of ${}^{b}Q$ -branch transitions and ${}^{a}R$ -branch transitions, along with a substantial number of ${}^{b}R$ -branch transitions with moderate intensities. The displacement of the Stark components were computed for the ${}^{b}Q$ -branch transitions and the ${}^{a}R$ -branch transitions using equation [2.15], a Stark voltage of 800 and a μ_a and μ_b of 0.5D. The results are summarized in Tables 17 and 18.

If μ_a and $\mu_b < 0.5D$ then it can be concluded, by reference to Equation [2.15], that in order to observe transitions of $SF_5 - N = C = O$ at a Stark voltage of 800V, the magnitude of the Stark coefficients, (A', B') and (A'', B'') must be greater than 1×10^{-6} and 3×10^{-7} respectively.

From the ${}^{b}Q$ -branch transitions, the displacement of the Stark components of the $6_{61} \leftarrow 6_{52}$, $7_{61} \leftarrow 7_{52}$ and $12_{66} \leftarrow 12_{57}$ transitions were calculated. The Stark components of these transitions were found to shift towards lower frequency. In order to observe a transition it is nec-

Table 17. Stark Shifts In Q-Branch Transitions.

Transition	*M*	Δν
$6_{61} \leftarrow 6_{52}$	6	-2.21
	4	-5.77
	2	-7.90
	1	-8.44
	0	-8.61
$7_{61} \leftarrow 7_{52}$	7	-0.09
	5	-4.44
	3	-7.34
	1	-8.79
	0	-8.97
$12_{66} \leftarrow 12_{57}$	12	-0.16
	9	-0.10
	6	-0.06
	3	-0.03
	0	-0.02

Table 18. Stark Shifts In R-Branch Transitions.

Transition	Δν				
	M = 0	M = 1	M = 2	M = 3	M = 4
$5_{05} \leftarrow 4_{04}$	0.38	0.76	4.16	9.83	17.76
$5_{14} \leftarrow 4_{13}$	−0.15	−46.96	−187.40	−421.46	−749.15
$5_{15} \leftarrow 4_{14}$	−0.44	45.85	184.71	416.16	740.18
$5_{23} \leftarrow 4_{22}$	−0.10	−0.11	−0.14	−0.17	−0.23
$5_{24} \leftarrow 4_{23}$	−0.10	−0.11	−0.14	−0.18	−0.23
$5_{32} \leftarrow 4_{31}$	1.05	1.00	0.83	0.56	0.17
$5_{33} \leftarrow 4_{32}$	1.05	1.00	0.83	0.56	0.17
$5_{41} \leftarrow 4_{40}$	1.01	0.94	0.71	0.33	−0.21
$5_{42} \leftarrow 4_{41}$	1.01	0.94	0.71	0.33	−0.21

essary for the Stark components to be shifted from the main line by at least 0.5 MHz and preferably by 1.0 MHz. Of these 3 transitions only the $6_{61} \leftarrow 6_{52}$ and the $7_{61} \leftarrow 7_{52}$ have sufficient Stark shifts to be observed. Therefore, of the 40 or more transitions lying within $\pm$ 1 MHz of a common center and expected to contribute to a very intense ${}^{b}Q$ − line, only the lowest 3 or 4 will actually be observable and no intense "pile up" is detected. A similar phenomenon occurs for the ${}^{a}R$ -branch transitions. The displacements of the Stark components for the $J = 5 \leftarrow J = 4$ transitions were calculated. As can be seen in Table 18 it would be quite difficult to observe all of these transitions since the Stark shifts are not sufficient in most cases. Only the $5_{05} \leftarrow 4_{04}$, $5_{15} \leftarrow 4_{14}$ and the $5_{14} \leftarrow 4_{13}$ transitions have reasonably significant Stark effects and can be resolved. In some cases when the Stark shifts are small, the Stark peak can fall on top of a nearby line peak, and thus cancel. For higher J values the situation is even less favorable since there will be more ${}^{a}R$ - transitions grouped together but only the 3 with $K_{-1} = 0,1$ will be observable.

4.3 *Assignment of the (S-32) Spectrum*

Due to the originally expected strong ${}^{b}Q$ and ${}^{a}R$ - bands not being observable and since the rotational transitions could not be assigned by considering their Stark shifts, the rotational transitions were assigned by correlating their line positions with those predicted from the electron diffraction model.

Initially, 5 transitions were selected and fitted to a rigid rotor model using a fitting program due to Kirchhoff [38]. These transitions consisted of ${}^{b}Q$ transitions for J = 6 and J = 7; an ${}^{a}R$ transition for $J = 8 \leftarrow 7$ and ${}^{b}R$ transition for $J = 5 \leftarrow 4$, and $J = 7 \leftarrow 6$. From the results of this first fit, more transitions could be predicted and transitions up to a J of 11 were included in the next fit. Further transitions were identified and transitions for still higher J's were incorporated into the fit. By continuing this "bootstrapping" approach, 26 transitions involving energy

levels up to a J of 18 were assigned. The assignments of these transitions is reasonable, however, is not conclusive. These assignments are summarized in Table 19. In Table 20, the rotational constants determined from this fit are presented.

Although only 26 of 501 observed transitions were included in the fit this is not a serious factor because;

1) Many of the transitions will involve energy levels having $J > 20$ where the effects of centrifugal distortion must be considered to obtain a good fit.

2) There will be vibrationally excited species which contribute to the spectrum.

Table 19. Assignment Of Transitions From The Rigid Rotor Fit.

Transition	Calc Freq	Obs Freq	Obs - Calc	Std Dev
$4_{40} \leftarrow 3_{31}$	20144.99	20145.80	0.81	0.26
$5_{15} \leftarrow 4_{04}$	13427.52	13428.57	1.05	0.16
$5_{23} \leftarrow 4_{14}$	16461.77	16462.23	0.46	0.17
$5_{32} \leftarrow 4_{23}$	19494.31	19493.03	−1.28	0.22
$5_{41} \leftarrow 4_{32}$	22527.34	22528.60	1.27	0.27
$5_{51} \leftarrow 5_{42}$	13648.62	13648.13	−0.50	0.27
$6_{06} \leftarrow 5_{05}$	14294.09	14293.30	−0.79	0.12
$6_{06} \leftarrow 5_{15}$	12778.30	12778.00	−0.30	0.13
$6_{16} \leftarrow 5_{05}$	15809.58	15809.18	−0.41	0.21
$6_{61} \leftarrow 6_{52}$	16681.65	16681.75	0.10	0.32
$7_{07} \leftarrow 6_{16}$	15160.94	15161.68	0.73	0.16
$7_{26} \leftarrow 6_{15}$	21224.96	21224.13	−0.83	0.26
$7_{34} \leftarrow 6_{25}$	24259.00	24259.10	0.10	0.25
$8_{08} \leftarrow 7_{17}$	17543.63	17544.62	0.99	0.20
$8_{17} \leftarrow 7_{16}$	19059.17	19058.29	−0.89	0.16
$9_{09} \leftarrow 8_{18}$	19926.37	19925.50	−0.87	0.25
$9_{18} \leftarrow 8_{27}$	16893.78	16893.90	0.12	0.29
$9_{28} \leftarrow 8_{35}$	13858.56	13858.30	−0.26	0.16
$10_{110} \leftarrow 9_{27}$	19271.26	19270.86	−0.41	0.43
$10_{28} \leftarrow 9_{37}$	16240.91	16240.80	−0.11	0.18
$10_{38} \leftarrow 9_{45}$	13207.88	13208.75	0.87	0.20
$12_{111} \leftarrow 11_{210}$	24042.43	24041.88	−0.55	0.49
$13_{49} \leftarrow 12_{58}$	17321.00	17321.90	−0.90	0.26
$14_{312} \leftarrow 13_{49}$	22737.28	22738.13	0.85	0.25
$15_{313} \leftarrow 14_{410}$	25119.62	25120.20	0.58	0.26
$18_{712} \leftarrow 17_{89}$	20134.56	20134.60	0.04	0.40
Average Standard Deviation = 0.243 MHz				

Table 20. Rotational Constants From The Rigid Rotor Fit.

	Experimental	Electron Diffraction
A	2707.69 ± 0.04	2704.68 ± 0.03
B	1191.22 ± 0.01	1192.58 ± 0.03
C	1191.13 ± 0.01	1191.88 ± 0.03

5.0 Summary And Conclusions

The rotational constants (A, B, C) determined from this study are very close to those determined by the electron diffraction study (Table 20) and on the basis of the 3 parameters alone cannot dispute the finding of a bent -N=C=O structure in the $SF_5 - N = C = O$ molecule. However, this is not conclusive. Due to lack of sufficient measurable Stark shifts, no dipole moment components (μ_g) were determined. The absence of any strong ^bQ and ^aR - bands in the low resolution spectrum and the significant reduction in the number of observable transition when the Stark voltage is lowered from 800V to 200V constitute strong evidence that the dipole moment of $SF_5 - N = C = O$ is less than 0.5D.

Further work will have to be done to confirm the structure. Investigation of the spectrum at higher Stark voltages can overcome the lack of observed Stark shifts, and allow the observation of additional transitions. This extension could not be done in this study due to instrument limitations. The Stark modulator used in this work could provide a maximum of 900V. Searching at several Stark voltages is also needed to locate more observable Stark shifts. Finally, to more conclusively determine the structure of $SF_5 - N = C = O$ at least 3 more reciprocal moments from other isotopic species (*i.e.*$^{34}SF_5 - N = C = O$) have to be

obtained. This is necessary because there are 6 unknown parameters (assuming the S-F bond lengths to be the same) to be determined and a minimum of 6 reciprocal moments are needed.

References

1. Eyster, Gillette, and Brockway, J. Am. Chem. Soc.,*62*, 3236 (1940).

2. Kimura, K., Katada, K., and Bauer, S. H., J. Am. Chem. Soc.,*88*, 416 (1966).

3. Hilderbrandt, R.L., and Bauer, S.H., J. Mol. Struc., *3*, 325 (1963).

4. Airey, W., Glidewell, C., Robiette, A.G., and Sheldrick, G.M., J. Mol. Struc., *8*, 435 (1971).

5. Murdoch, J.D., Rankin, D.W.H., and Beagley, B., J. Mol. Struc., *31*, 291 (1976).

6. Rankin, D.W.H., and Cyvin, S.J., J. Chem. Soc. Dalton, 1277 (1972).

7. Curl, R.F., Rao, V.M., Sastry, V.L.N., and Hodgeson, J.A., J. Chem. Phys.,*39,(12)*, 3335 (1963).

8. Lett, R.G., and Flygare, W.H., J. Chem. Phys.,*17,(11)*, 4730 (1967).

9. Beard, C.I., and Dailey, B.P., *Technical Report*, No. 79 (1948).

10. Kirby, C. and Kroto, H.W., J. Mol. Spectrosc.,*70*, 216 (1978).

11. Durig, J.R., Nease, A.B., Berry, R.J., Sullivan, J.F., Li, Y.S., and Wurrey, J.R., J. Chem. Phys.,*84,(7)*, 3663 (1986).

12. Gerry, M.C.L., Thompson, J.C., and Sugden, T.M., Nature,*211*, 846 (1966).

13. Hocking, W. H., and Gerry, M. C. L., J. Mol. Spectrosc.,*42*, 547 (1972).

14. Yamada, K., Winnewisser, M., Winnewisser, G., Szalanski, L.B., and Gerry, M.C.L., J. Mol. Spectrosc.*79*, 295 (1980)

15. Yamada, K. J. Mol. Spectrosc.,*79*, 323 (1980).

16. Oberhammer, H., Z. Naturforsch.,*26a*, 280 (1971).

17. Oberhammer, H., Seppelt, K., and Mews, R., J. Mol. Struc.,*101*, 326 (1983).

18. Rode, B.M., Kosmus, W., and Nachbaur, E., Chem. Phys. Lett.,*17,(2)*, 186 (1972).

19. Kosmus, W., Rode, B.M., and Nachbauer, E., J. Elec. Spectrosc.,*1*, 408 (1972/73).

20. McLean, A. D., Loew, G. H., and Berkowitz, D. S., J. Mol. Spectrosc.,*64*, 184 (1977).

21. Rode, B.M., Kosmus, W., and Nachbaur, E., Monatsh. Chemie,*105*, 191 (1974).

22. Rode, B.M., Kosmus, W., and Nachbaur, E., Z. Naturforsch.,*29a*, 650 (1974).

23. Thrasher, J.S., Private Communication. (1985).

24. Levine, I. N., *Molecular Spectroscopy,*, Wiley Interscience, New York, 1975.

25. Townes, C. H., and Schawlow, A. L., *Microwave Spectroscopy,*, McGraw-Hill Book Co., Inc., New York, 1955.

26. Gordy, W., and Cook, R. L., *Microwave Molecular Spectra,*, Vol. IX, John Wiley and Sons, Inc., New York, 1970

27. King, G. W., Hainer, R. M., and Cross, P. C., J. Chem. Phys.,*11*, 27 (1943).

28. Sugden, T. M., and Kenney, C. N., *Microwave Spectroscopy of Gases,*, D. Van Nostrand Co., Ltd., London, 1965.

29. Wollrab, J. E., *Rotational Spectra and Molecular Structure,*, Academic Press, New York, 1967.

30. Straughan, B. P., and Walker, S., *Spectroscopy,*, Vol. 2, Chapman and Hall Ltd., London, 1976.

31. Duncan, L. C., Rhyne, T. C., Clifford, A. F., Shaddix, R. E., and Thompson, J. W., J. Inorg. Nucl. Chem., Suppl., (1967).

32. Botschwina, P., Nachbaur, E., and Rode, B. M., Chem. Phys. Lett.,*41*, 486 (1976).

33. Poppinger, D., Radom, L., and Pople, J. A., J. Am. Chem. Soc.,*99*, 7806 (1977).

34. McLean, A. D., Loew, G. H., and Berkowitz, D. S., J. Mol. Spectrosc.,*72*, 430 (1978).

35. Gordy, W., Smith, W. V., and Trambarulo, R. E., *Microwave Spectroscopy,*, John Wiley and Sons, Inc., New York, 1953.

36. Tullock, W.C., Coffman, D.D., and Muetterties, E.L., J. Am. Chem. Soc.,*86*, 357 (1964).

37. Kirchhoff, W.H., and Wilson, E.B., Jr., J. Am. Chem. Soc.,*84*, 334 (1962).

38. Kirchhoff, W.H., J. Mol. Spectrosc.,*41,(2)*, 333 (1972).

The vita has been removed
from the scanned document